Structural Analyses of Triacylglycerol Polymorphs with FT-IR Techniques. 1. Assignments of CH_2 Progression Bands of Saturated Monoacid Triacylglycerols

Junko Yano, Fumitoshi Kaneko,* and Masamichi Kobayashi

Department of Macromolecular Science, Graduate School of Science, Osaka University, Toyonaka 560, Japan

Kiyotaka Sato

Faculty of Applied Biological Science, Hiroshima University, Higashi-Hiroshima 739, Japan

Received: April 15, 1997; In Final Form: July 21, 1997[⊗]

As the first step for full assignment of infrared (IR) active vibrational modes in crystalline triacylglycerols (TAGs), methylene wagging and rocking regions of β-forms of a series of monoacid TAGs having C10 through C22 acids were investigated. The wagging region was especially complicated, because dispersion curves of methylene wagging (ν_3) and twisting−rocking (ν_7) modes were overlapped and the three acyl chains of TAGs exhibited their own IR bands. In order to resolve the complicated spectra of TAGs, three polarized IR techniques (oblique transmission, attenuated total reflection, and reflection-absorption spectroscopy) were employed in addition to the ordinary transmission method, and the obtained spectra were compared with those of a series of monoacid 1,3-diacylglycerols. It was found that the two straight *sn*-1 and *sn*-2 chains of monoacid TAGs showed different series of IR progression bands from those of the bend *sn*-3 chain having a *gauche* bond in the neighborhood of the ester bond. The ν_7 modes of the bend chain made a significant contribution to the CH_2 wagging region as well as the ν_3 modes of both the straight chains and the bent chain.

Introduction

Triacylglycerols (TAGs) are main components of fat products and major energy storage lipids in plants and higher animals. In the fat products, macroscopic properties, such as texture, plasticity, rheology, and morphology, are influenced by molecular conformation of TAGs present in emulsions and membranes and by their crystal structures in solid phases.[1−4] Despite its importance, the molecular level understanding of structure−function relationships of TAGs having various types of saturated and unsaturated fatty acid moieties has still been open to question.

The best way to clarify molecular-level structures is X-ray crystal structure analysis using high-quality single crystals. In TAGs, however, it is usually difficult to grow proper single-crystal specimens, because of influences of complicated polymorphism, lattice defects, impurities, and so on. Therefore, very limited results have been obtained for the most stable polymorphs, β-forms of trilaurin,[5] tricaprin,[6] and 1,2-dipalmitoyl-3-acetyl-*sn*-glycerol.[7] As to metastable forms such as β- and α-forms whose properties are often more functional than those of β-forms, single crystals can hardly be grown due to thermodynamical metastability. Therefore, the powder X-ray diffraction method has been used for the polymorphic studies of TAGs. Using this method, we can obtain information about subcell structure and long spacing, but yet local structural information such as molecular conformation and orientation of functional groups is not available.

Vibrational spectroscopy has a potential to compensate this weak point of powder X-ray diffraction. Vibrational spectra are sensitive to molecular conformation and subcell structure and can be measured under various conditions of specimens, such as membranes, powders, crystals, and so on. If an oriented specimen can be prepared, the following information also becomes available: (1) structure and orientation of functional groups, (2) dynamical properties, (3) conformational and orientational disorders, and (4) subcell orientation.[8] In addition, the recent development of spectrometers for vibrational spectroscopy is remarkable. We noticed the high performance of FT-IR spectrometers; polarized spectra can be taken quite easily using a small single-crystal specimen. Many techniques for FT-IR spectroscopy also have been developed; diffuse reflection spectroscopy, attenuated total reflection (ATR) spectroscopy,[9] reflection absorption spectroscopy (RAS),[10−12] and so on.

In previous studies on TAGs, the above advantages of vibrational spectroscopy have not been fully utilized. In most cases, it was used to determine subcell structure and/or to distinguish polymorphic forms.[13−15] It seems that the lack of basic information about the relationship between structure and spectrum prevents the positive utilization of vibrational spectroscopy. As for this problem, the infrared CH_2 wagging (1400−1150 cm^{-1}) and CH_2 rocking (1000−700 cm^{-1}) regions have been studied in detail for *n*-alkanes, *n*-alcohols, and *n*-fatty acids,[16−26] and it has been clarified that the CH_2 progression bands are sensitive to chain length and molecular conformation. Although the CH_2 wagging modes of TAGs have been studied earlier, the assignments are still uncertain.[15]

We tried to assign the bands in the CH_2 wagging and CH_2 rocking regions. The problem we met soon was the complexity of these regions, which could be attributed to the following two causes. Dispersion curves of CH_2 wagging modes and twisting−rocking modes (ν_3 and ν_7 branches) were overlapped in the CH_2 wagging region and those of CH_2 rocking−twisting modes and C−C stretch modes (ν_8 and ν_4 branches) in the CH_2 rocking region.

In addition, the modes of the three acyl chains of TAGs are distributed in the same frequency region. To resolve the complicated spectra of TAGs, we studied them in the following ways.

* Corresponding author. Fax: +81-6-850-5453.

[⊗] Abstract published in *Advance ACS Abstracts,* September 15, 1997.

S1089-5647(97)01304-7 CCC: $14.00

(1) We considered that the employment of specimens of β-forms whose structures can easily be assessed on the basis of X-ray single-crystal data[5,6] is necessary for making detailed assignment and understanding the relationship between IR spectra and molecular and crystal structures of TAGs. With solution grown single-crystal specimens of β-forms, we tried to assign the bands in the CH_2 wagging and CH_2 rocking regions.

(2) According to the previous studies on *n*-alkanes and *n*-alcohols,[22,25] the chain length dependence of frequencies of progression bands was investigated systematically with a series of even-numbered monoacid TAGs consisting of C12 acid to C22 acid.

(3) In the β-forms of monoacid TAGs, one of the three acyl chains takes the *gauche* conformation in the vicinity of the glycerol backbone.[5,6] To distinguish the bands of the straight chains from those of the bend chain, IR spectra of a series of monoacid 1,3-diacylglycerols (DAGs) whose two acyl chains take the all-*trans* conformation[27,28] were measured and were compared with those of monoacid TAGs.

(4) To reduce band width due to thermal fluctuation, some spectra were measured with specimens cooled with liquid N_2.

(5) We considered that the modes of the ν_3 and ν_7 branches were distributed in the same frequency region but the direction of transition moments would be different between them. Therefore, we took polarization measurements seriously. Polarized spectra were measured by ordinary normal transmission, oblique transmission,[29,30] ATR,[9] and RAS methods.[10−12] The latter three techniques make three-dimensional polarization analysis possible, which was very useful in this study as described below.

With this study plan we could analyze the spectra in the CH_2 wagging and CH_2 rocking regions of monoacid TAGs. We found that the experimental methods and the results were useful for the polymorphic studies of TAGs and applied to asymmetric TAGs. In this paper, we deal with the experiment and analyses and the obtained assignments of monoacid TAGs. The application will be treated in the following paper (Part 2).

Background

1. Progression Bands of Long-Chain Compounds. Vibrational spectra of long-chain molecules have been interpreted on the basis of the vibrational modes of an infinite polymethylene chain.[22−25] Molecular vibrations of the all-*trans* hydrocarbon chains of a certain finite length are approximated by the modes on the dispersion curves (the frequencies ν as a function of the phase angle δ between the neighboring methylene units) of the infinitely extended polymethylene chain. Only the vibrational modes at $\delta = 0$ or π are infrared and/or Raman active for the infinite chain. In case of the finite chain, the modes of $\delta = 0$ and π become optically active and a series of bands, namely progression bands, appear in IR and/or Raman spectra.

The allowed phase angles for the finite chains can be obtained using the simple coupled oscillator approximation. For a chain having *N* oscillators, the modes of the following phase angles are allowed

$$\delta = k\pi/(N+1), \quad k = 1, 2, 3, ..., N \qquad (1)$$

In this study we have focused on the progression bands of ν_3, ν_7, and ν_8 branches whose frequencies change significantly with phase angle, as shown in Figure 1. The length and conformation of hydrocarbon chains are reflected in the frequencies of these progression bands sensitively. Since the

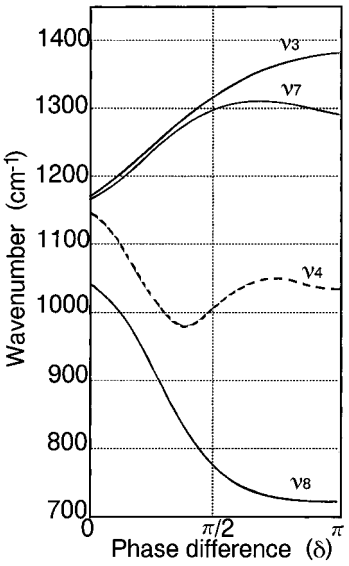

Figure 1. Dispersion curves for a polymethylene chain. The branches drawn with solid lines are treated in this paper.[23,24]

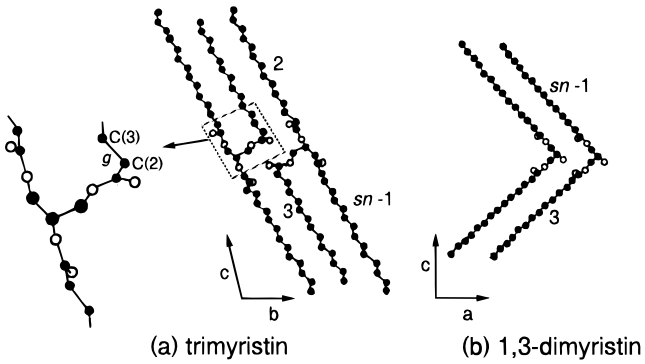

Figure 2. (a) Molecular model of the β-form of trimyristin, built with reference to the X-ray structure analyses of the β-forms of tricaprin and trilaurin.[5,6] (b) Molecular model of *sn*-1,3-dimyristin, built with reference to the X-ray structure analyses of 1,3-DAG of 11-bromoundecanoic acid[27] and 1,3-DAG of 3-thiadodecanoic acid.[28]

ν_3 modes mainly arise from the CH_2 wagging modes, their polarization directions are parallel to the chain axis. In the ν_7 and ν_8 modes, the coupling between twisting and rocking is remarkable. At $\delta = 0$, the ν_7 mode is pure rocking and the ν_8 mode is pure twisting. As the phase angle increases, the mixing of rocking and twisting occurs. Finally, the assignments are reversed at $\delta = \pi$; ν_7 is pure twisting and ν_8 is pure rocking.

2. Crystal Structure of β-Forms of Monoacid TAGs.[5,6] The space group is $P\bar{1}$, which has a center of symmetry, and the unit cell contains two molecules in two isotypic forms. The chains are packed with zigzag planes parallel to each other according to triclinic subcell ($T_{||}$) (Figure 2a). In three acyl chains, two of them are straight with the all-*trans* conformation and the third chain has bent conformation with *gauche* bond between C(2) and C(3) in the *sn*-3 acyl chain.

Experiments

Samples. Even-numbered monoacid TAGs of tricaprin (Nc = 10) through tribehenin (Nc = 22) and even-numbered monoacid 1,3-diacylglycerols (1,3-DAGs) of dicaprin (Nc = 10) through diarachidin (Nc = 20) were purchased from Sigma Co., Ltd. The purity was higher than 99% for the all materials. Single crystals of β-forms of TAGs and 1,3-DAGs were crystallized from *n*-hexane solution by slow cooling.

In this paper, we have used the words "TAGs" and "DAGs" as the meanings of monoacid-triacylglycerols and monoacid-diacylglycerols.

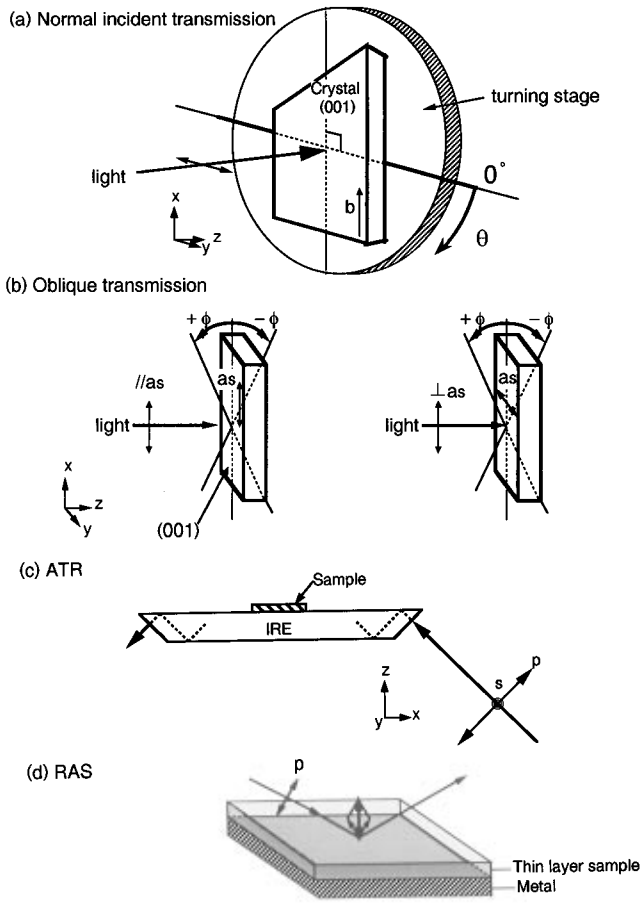

Figure 3. Schematic representation of (a) the normal incident transmission, (b) the oblique transmission method, (c) ATR, and (d) RAS.

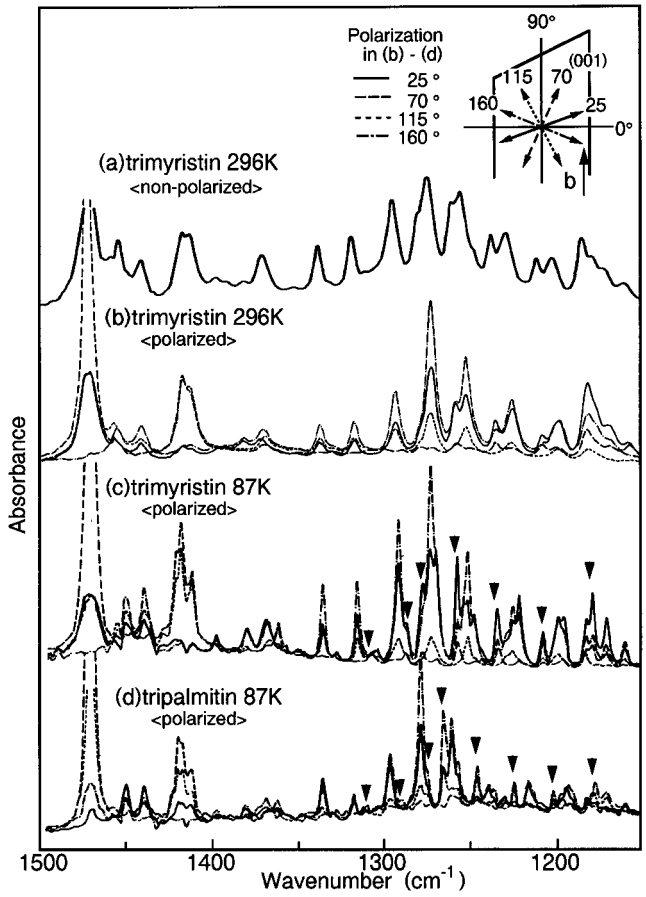

Figure 4. Normal incident transmission spectra of the β-forms: nonpolarized spectrum of trimyristin measured at 296 K (a), polarized spectra of trimyristin measured at 296 K (b) and 87 K (c), and that of tripalmitin measured at 87 K (d). The relationship between the polarization of incident radiation and the crystal morphology is schematically shown at the top right. The bands marked with arrows are the ν_7 progression bands of the *sn*-3 chains.

Measurements. The transmission IR spectra were taken with Degilab FTS60A spectrometer. As for RAS and ATR measurements, we employed a JASCO FT-IR 8300 spectrometer and its accessories. For measurement at low temperatures, an Oxford flow type cryostat CF1104 and an Oxford temperature controller ITC-4 were used. Small-sized crystal samples were measured with a JASCO Janssen Micro FT-IR spectrometer. The polarized IR spectra were measured with a MCT detector and a wire-grid polarizer (JASCO PR500).

To obtain three-dimensional structural information, the following IR techniques were used.

1. Polarized IR Transmission Methods. Normal incident transmission spectra and oblique transmission spectra were taken in the present study.[29,30]

As for the former case, the direction of IR radiation was normal to the (001) plane of the crystal, as shown in Figure 3a. The direction of the electric field of the incident radiation was fixed, and the sample was rotated about the normal of the (001) plane. In this study, we assumed that the *b*-axis of crystals is parallel to the 90° polarization direction. In this case, the information deduced from the polarization dependence of the IR spectra concerns the projection of transition moments onto the (001) plane. No three-dimensional information is available by this technique.

The oblique transmission method has been developed to overcome the above limit of the normal incident method.[29,30] The specimen was tilted with angle of ϕ shown in Figure 3b.

2. ATR.[9] The transmission method cannot be applied for thick specimens or strong absorption bands. In such a case, the ATR method is useful. In this study the flat (001) plane of specimens was set on the sampling plane of an internal reflection element (IRE) of ZnSe whose wedge angle was 45°, and reflection spectra were measured with p- or s-polarized incident radiation as shown in Figure 3c. With p-polarization the *x* and *z*-components of a transition moment are observed, and the *y*-component with s-polarization. With the above conditions the *z*-component that cannot be observed with the normal incident transmission method is enhanced in the p-polarized spectra.

By the combination of the p- and s-polarization measurements, three-dimensional structural information can be obtained. Using this property we investigated the direction of transition moments.

3. RAS.[10−12] Since a strong electric field normal to the metal surface is generated in this method as shown in Figure 3d, the modes of this direction are observed selectively. Samples were built up on a metal surface as a thin film where the lamellar interface is parallel to the metal surface by developing chloroform solution. Accordingly, the bands whose transition moments are parallel to the chain axis are emphasized.

Results and Discussion

1. Assignments of IR Bands in 1360−1150 cm^{-1} Region. Figure 4 and Table 1 show the normal incident transmission spectra and the frequencies of trimyristin and tripalmitin measured with the nonpolarized and polarized IR beams. In the polarization measurements, the sample setting was chosen so that the electric field of the 0° polarization was perpendicular to the long edge of single crystal, which corresponds to the

TABLE 1: Frequencies and Assignments of Bands in the CH_2 Wagging Region of Trimyristin and Tripalmitin[a]

trimyristin			tripalmitin		
transmission[b] (cm^{-1})	RAS (cm^{-1})	assignment[d]	transmission[b] (cm^{-1})	RAS (cm^{-1})	assignment[d]
1163.3(w)			1163.2(vw)		
1174.0(m)		T1-t	1174.0(w)		T1-t
1182.3(m)	1182.5	W1-t	1181.2(m)	1182.5	W1-t
1185.3(m)		T1-g	1185.5(w)		T1-g
1198.6(m)		W1-g	1194.6(m)		
1202.4(m)	1202.8	W2-t	1197.2(m)	1197.9	W1-g
1210.5(m)		T2-g	1200.3(m)		W2-t
1224.7(m)		T3-t	1204.7(m)		T2-g
1228.4(m)		W2-g	1213.2(vw)		T3-t
1231.0(w)	1229.8	W3-t	1216.8(m)		W2-g
1237.1(m)		T3-g	1219.5(m)	1222.1	W3-t
1246.3(vw)		T4-t	1227.8(m)		T3-g
1250.5(m)			1233.6(w)		
1254.8(S)		W3-g	1239.0(m)		T4-t
1257.0(m)	1256.8	W4-t	1242.2(m)	1246.0	W3-g
1260.6(S)		T4-g		1247.6	W4-t
1272.6(S)		T5-t	1249.2(m)		T4-g
1275.8(S)	1274.6	W4-g	1260.7(m)		T5-t
1280.0(S)	1280.4	W5-t,T5-g	1263.3(S)		W4-g
1290.1(m)		T6-g	1268.8(S)	1266.9	W5-t,T5-g
1295.7(S)	1294.4	W5-g	1278.3(m)		T6-g
	1301.6		1282.1(S)	1280.9	W5-g
1306.8(vw)	sh[c]	W6-t	1287.3(vw)	1287.2	W6-t
1311.0(vw)			1300.3(S)	1300.7	W6-g
1319.2(S)	1319.0	W6-g	1306.9(vw)	1304.0	W7-t
1331.4(vw)	1331.0	W7-t	1313.6(vw)	1312.7	
1339.3(S)	1339.0	W7-g	1321.4(m)	1320.9	W7-g
1351.1(vw)	1349.9	W8-t	1331.9(vw)	1331.0	W8-t
			1339.6(m)		W8-g
			1349.5(vw)	1348.4	W9-t

[a] The frequencies of bands are of the polarized transmission spectra measured at 87 K (Figure 4c,d) and RAS measured at 296 K. [b] S, strong; m, medium, w, weak; vw, very weak. [c] sh, shoulder. [d] W, ν_3 mode; T, ν_7 mode; t, straight *sn*-1,2 chains; g, bent *sn*-3 chain.

b-axis of the crystal unit cell. Figure 4a,b shows the nonpolarized and polarized spectra of trimyristin taken at 296 K. The polarization measurement made frequencies and polarization properties of each band clear. However, separation of each specific band was not satisfactory at room temperature (Figure 4b) due to thermal fluctuation. By cooling specimens to a low enough temperature, we could measure the frequency of each band definitely (Figure 4c,d).

The spectra in the methylene wagging region (1360−1150 cm^{-1}) are complicated in TAGs. In the previous work of β-forms of *n*-alcohols, their complicated features in the wagging region were interpreted as superposition of the ν_3 and ν_7 progression bands arising from two types of molecules in the unit cell, straight molecules and bent ones.[25] Similarly, we analyzed the TAG spectra by taking into account two types of acyl chains in the following manner: (1) contribution of ν_7 and ν_3 branches and (2) contribution of straight (*sn*-1,2) and bent (*sn*-3) acyl chains (see Figure 2a). Hence, it follows that at least four types of progression bands may overlap in this region, e.g., the ν_7 and ν_3 branches of straight and bent chains. As to the first point, we noticed the difference in the direction of transition dipole moments between the ν_3 and ν_7 modes. Then, the modes due to the *sn*-1,2 chains were differentiated from those due to the *sn*-3 chain by difference to *sn*-1,3 diacylglycerols in Figure 2b. The chain-length dependence of the ν_3 and ν_7 modes was also investigated in detail, as studied in the previous studies.

Assignments of ν_3 Bands. The first step was to distinguish two types of progression bands: ν_3 and ν_7. Since the CH_2 wagging mode has a transition dipole moment parallel to the hydrocarbon chain axis, the transition moments of the ν_3 progression bands have a large component parallel to the chain axis. On the other hand, the ν_7 progression bands include the perpendicular component with respect to the chain axis, since the transition moments of the CH_2 rocking modes are perpendicular to the skeletal plane of hydrocarbon chains. Utilizing these polarization characteristics of the ν_3 and ν_7 modes seems to be useful for the assignment. Judging from the crystal structure of β, IR bands having a large perpendicular component are emphasized when single-crystal specimens are measured with the ordinary normal incident transmission method. However, as long as only the normal incidence is employed, we cannot judge precisely whether a transition moment is parallel or perpendicular to the chain axis. The projections of transition moments onto the basal plane can be obtained. Information about transition moments perpendicular to the basal plane is necessary for the precise judgment. For this purpose, we employed RAS (Figure 5), the oblique IR transmission method (Figure 6), and ATR (Figure 7).

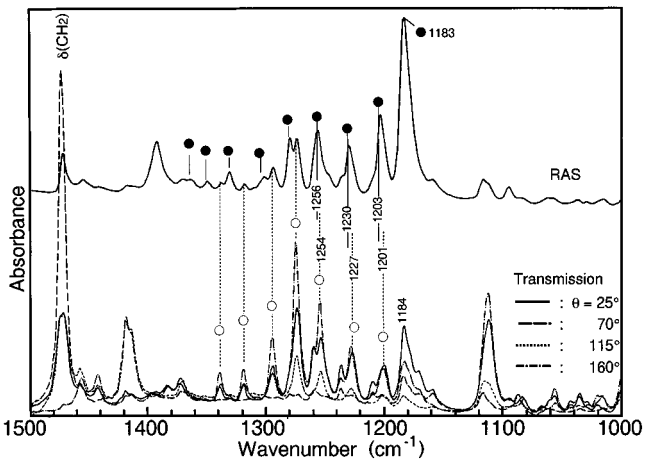

Figure 5. Normal incident transmission (lower) and RAS (upper) spectra of trimyristin. The bands marked with closed circles are detectable only in RAS. On the other hand, the bands with open circles appear more intense in the transmission spectra.

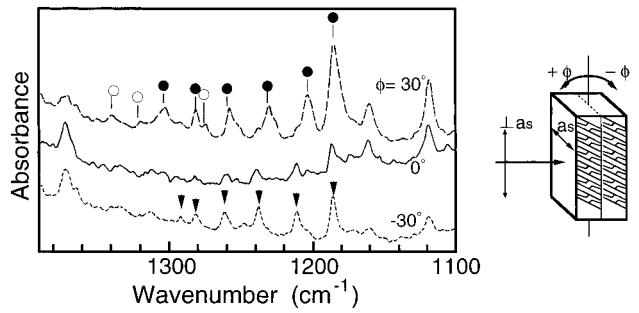

Figure 6. Infrared spectra of trimyristin measured with the oblique transmission method.

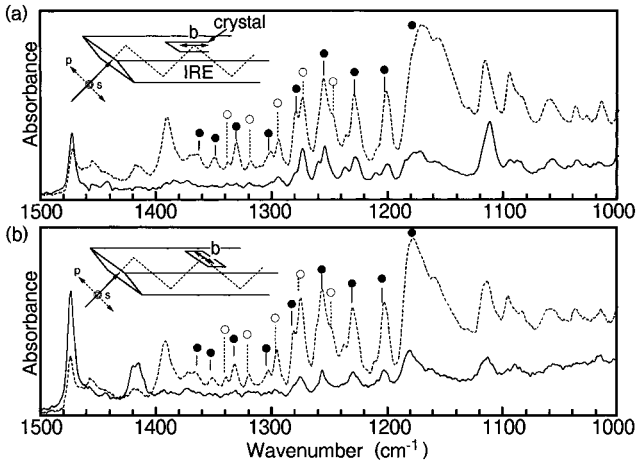

Figure 7. Polarized ATR spectra of trimyristin taken on the (001) face of the crystal. The *b*-axis is set parallel to the scattering plane in (a), and that is set perpendicular to the scattering plane in (b). s-Polarized spectra and p-polarized ones are drawn with solid and dotted lines, respectively.

Figure 5 shows the transmission and RAS spectra of trimyristin measured at room temperature. We confirmed by comparing IR spectra that the thin layer specimen used for RAS was the β-phase; for example, the $\delta(CH_2)$ band appeared as singlet as 1472 cm^{-1}, which is the feature of β having a $T_{\parallel}$ subcell.[14] The difference in the intensity of $\delta(CH_2)$ band between RAS and transmission spectra is a proof of the normal arrangement of TAG molecules with respect to the metal surface in the thin layer sample for RAS. The $\delta(CH_2)$ band in RAS spectra was quite weak compared with that in transmission spectra, which strongly suggests that the lamellar interface was parallel to the metal surface. Accordingly, vibrational modes perpendicular to the (001) plane were observed strongly in RAS. In the region of 1360−1150 cm^{-1}, the bands marked with closed circles were emphasized in RAS. On the other hand, some bands with open circles appear in both of the transmission spectra and RAS. As to the lower four bands in RAS, the frequencies do not equal to the corresponding bands in the transmission spectra. Except for the first bands at 1183 cm^{-1}, the next three bands have slightly higher frequencies. As mentioned in Figure 4b,c, the bands taken at room temperature include several components. Therefore, the higher frequencies of the three bands in RAS are due to the contribution of the higher component in each band. We inferred from the results that the observed bands in RAS consist of two series of progression bands, one of which mainly includes the perpendicular component to the (001) plane and another has both of perpendicular and parallel components. The lower bands will arise from the overlapping of these two types of progression bands, mainly from the former one. We expected that those

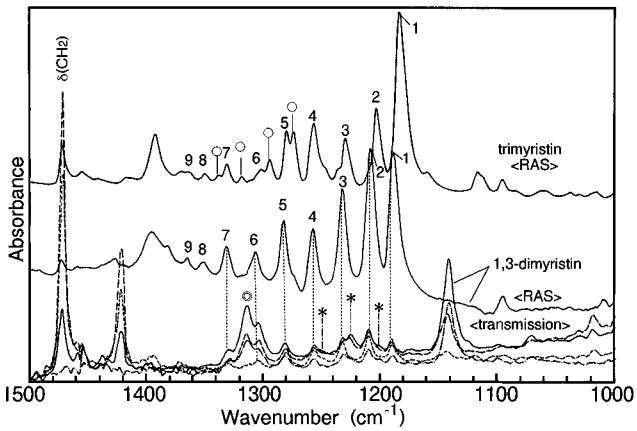

Figure 8. Normal incident transmission and RAS spectra of 1,3-dimyristin (bottom and middle) and RAS spectrum of trimyristin (top). The band with a double circle around 1310 cm^{-1} in the transmission spectra of 1,3-dimyristin is common to all 1,3-DAGs and may be the band arising from OH groups.

two types of progression bands are of the ν_3 modes, one of which is of the straight *sn*-1,2 chains and another of the bent *sn*-3 chains.

Intensity changes in oblique and ATR spectra support the result obtained in RAS. Figure 6 shows the oblique transmission spectra of trimyristin taken at 296 K. In the oblique transmission method, the arrangement of the specimen is determined with two setting angles, θ and ϕ. In this measurement, the crystal was set at $\theta = 70°$, where the $\delta(CH_2)$ band showed the strongest absorption. The bands in the CH_2 wagging region change appreciably in intensity with an alternation of the angle of inclination ϕ. The bands marked with closed circles increase in intensity at $\phi = 30°$, while another series of bands with arrows emerge at $\phi = -30°$. The former bands correspond to the bands in RAS spectra (Figure 5) and also appear appreciably in p-polarized ATR spectra (Figure 7). Irrespective of the arrangement of the single-crystal specimen on IRE, these bands exhibit strong absorption. Considering the tilting direction of hydrocarbon chains, the parallel bands to the chain axis become intense at $\phi = +30°$ and the perpendicular bands at $\phi = -30°$. This was confirmed by measuring the intensity change of the $\delta(CH_2)$ band. Consequently, the bands with closed circles can be assigned to the ν_3 progression bands, and the bands with arrows to the ν_7 ones. We will discuss assignment of the ν_7 bands later.

To identify the bands of straight *sn*-1,2 chains, we compared the spectra of TAGs with those of 1,3-DAGs whose two hydrocarbon chains took an all-*trans* conformation (Figure 2b). Figure 8 shows the transmission spectra of 1,3-dimyristin and RAS of 1,3-dimyristin and trimyristin. The bands numbered from 1 through 9 of trimyristin coincide well with those of 1,3-dimyristin. As for the first three wagging modes ($k = 1-3$), however, a deviation in frequency is not negligible. The CH_2 wagging modes are strongly coupled with the C−O stretch mode of the carboxyl group esterified with the glycerol backbone.[25,31] We inferred that the deviation may reflect the difference in conformation of the glycerol moiety between TAGs and 1,3−DAGs. Consequently, we assigned the bands numbered from 1 through 9 to the ν_3 progression bands of the straight *sn*-1,2 chains.

In the same way, we have compared TAGs (Nc = 10−22) with 1,3-DAGs (Nc = 12−20). Figure 9a shows the band positions of the TAGs observed in transmission spectra taken at 87 K. The solid lines indicate the ν_3 bands of the straight *sn*-1,2 chains. Another series of the progression bands having both perpendicular and parallel components was connected by

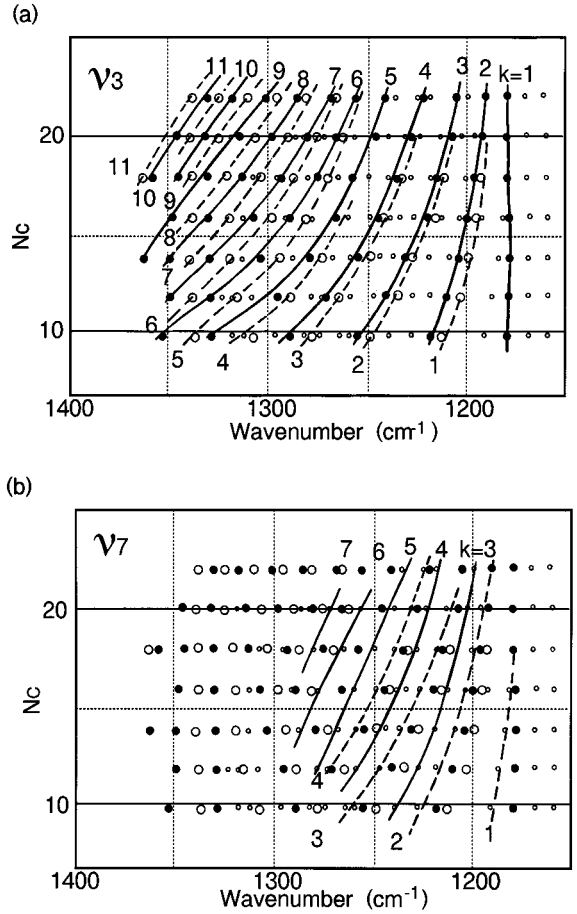

Figure 9. (a) ν_3 branch mode array for monoacid TAGs of tricaprin (Nc = 10) through tribehenin (Nc = 22). Solid lines with closed circles, straight *sn*-1,2 chains; broken lines with open circles, bent *sn*-3 chain. (b) ν_7 branch mode array for monoacid TAGs (small open circles). Solid lines, straight *sn*-1,2 chains; broken lines, bent *sn*-3 chain. All frequency data were obtained at 87 K by the normal incident transmission method.

dotted lines. These bands can be assigned to the ν_3 progression bands of the bent *sn*-3 chains, because of the following reasons.

(1) The region where these bands appear extends beyond 1350 cm^{-1} as the theoretical curve for the ν_3 branch, whereas the maximum of the ν_7 branch is about 1310 cm^{-1} (Figure 1).

(2) In addition to point 1, the possibility of ν_3 bands of the straight chains is denied because 1,3-dimyristin did not have such outstanding bands in both the transmission spectra and RAS.

(3) In Figure 8, the marked bands with open circles of trimyristin are not observed in 1,3-dimyristin; namely, it is typical for bent chain conformation of TAGs.

(4) These bands have a tendency to appear at slightly higher frequencies than the ν_3 bands of the straight *sn*-1,2 chains. This may be the influence of the bent conformation of *sn*-3 chains, in which the theoretical number of oscillators is one less than that of the straight chains because of the inserted *gauche* bond near the esterified moiety.

Assignments of ν_7 Bands. Unassigned bands to the ν_3 branch in Figure 9a will arise from the ν_7 branch of both the straight and bent chains. Therefore, our next task is to draw a distinction between ν_7 bands of the straight chains and those of the bent chains. Consulting the IR spectra of *n*-alkanes and *n*-alcohols, the ν_7 bands have very weak intensity in the case in which the acyl chains have all-*trans* conformation.[22,25] In the same manner as those molecules, some bands (indicated by * in Figure 8) with very weak intensity appear in the transmission spectra of 1,3-DAGs. In the case of TAGs, however, a series of outstanding bands was observed in the transmission spectra as shown in Figure 4. These bands with arrows in Figure 4 were also observed in the oblique transmission spectra in Figure 6, and the intensity was increased on tilting the specimen toward $\phi = -30°$. Namely, the direction of the transition dipole moment of these bands is parallel to the molecular chain axis. These bands were connected by dotted lines in Figure 9b. We concluded to assign the bands to the ν_7 of the bent *sn*-3 chains. It is because of the two reasons: (1) these bands were observed in the limited region of 1310−1150 cm^{-1}, and (2) 1,3-dimyristin with an all-*trans* conformation did not have any strong ν_7 bands.

Finally, the progression bands having the weakest intensity, which were assigned neither to the ν_3 bands of the *sn*-1,2 and *sn*-3 chains nor to the ν_7 bands of the *sn*-3 chains, were assigned to the ν_7 bands of the straight *sn*-1,2 chains.

Comparison of the Experimental Results with Theoretical Dispersion Curves. In order to confirm the assignments of the ν_3 and ν_7 progression bands, we compared the observed frequencies with theoretical dispersion curves with the help of a simple coupled oscillator model. For the straight *sn*-1,2 chains consisting of Nc carbon atoms, the number of oscillators (namely, the number of methylene groups) is Nc − 2. By substituting Nc − 2 for *N* of eq 1, the allowed phase angles of the *sn*-1,2 chains ($\delta_{k,sn\text{-}1,2}$) can be expressed as

$$\delta_{k,sn\text{-}1,2} = k\pi/(\mathrm{Nc} - 1), \quad k = 1, 2, ..., \mathrm{Nc} - 2 \qquad (2)$$

For the bent chains, we assumed that the number of oscillators is one methylene group less than that of the *sn*-1,2 chain, namely, Nc − 3, because of the insertion of a *gauche* bond between C(2) and C(3) (see Figure 2a). Therefore, the allowed phase angles of the *sn*-3 chain ($\delta_{k,sn\text{-}3}$) can be expressed as

$$\delta_{k,sn\text{-}3} = \mathrm{k}\pi/(\mathrm{Nc} - 2), \quad k = 1, 2, ..., \mathrm{Nc} - 3 \qquad (3)$$

Figure 10a shows a plot of the observed frequencies of the ν_3 bands against the allowed phase angles, comparing with the theoretically obtained ν_3 dispersion curve. The observed frequency data agree well with the ν_3 dispersion curve, which strongly supports our assignment of the ν_3 bands. Similarly, the experimental data of the ν_7 dispersion bands also coincide well with the ν_7 dispersion curve in Figure 10b, except several ambiguities with regard to the values of *k*. Since the dispersion of the ν_7 branch is quite small in the region of $\pi/2 < \delta < \pi$, we could not determine the *k* values of the bands around 1300 cm^{-1}. Another cause of the ambiguities is the existence of the asymmetric C−O stretch (ν(C−O)) bands in the region of 1180−1150 cm^{-1}.[15,25,31]

For the assignments of the bands due to the bent *sn*-3 chains, we applied the number of methylene groups in the all-*trans* moiety (Nc − 2) to the simple coupled oscillator model. This treatment worked well as the first approximation, but there are small deviations from theoretical dispersion curves, probably due to the terminal group effect of the bent moiety. We also found that the bent portion had an influence on the intensity and polarization of the progression bands. As described before, the ν_7 progression bands due to the straight *sn*-1,2 chains are weak, while those due to the bent *sn*-3 chains appear with pronounced intensities. We consider that the arrangement of the C−O group at the esterified moiety with respect to the all-*trans* hydrocarbon portion relates to this phenomenon.

For the straight acyl chain, the C−O bond at the esterified portion is almost parallel to the chain axis and is coplanar with the hydrocarbon zigzag plane. Therefore, the wagging modes whose transition moments are parallel to the chain axis can couple with the ν(C−O) mode and borrow its intensity. For example, in fatty acids and their derivatives having all-*trans*

TABLE 2: Frequencies and Assignments of Bands in the CH_2 Rocking Region of Trimyristin, Tripalmitin, 1,3-Dimyristin, and 1,3-Dipalmitin Measured at 87 K (Figure 11).

trimyristin			tripalmitin		
transmission (cm^{-1})	assignment[a]	transmission (cm^{-1})	transmission (cm^{-1})	assignment[a]	transmission (cm^{-1})
899.2	r(CH_3),r4-t	902.4	897.0	r(CH_3)	
891.2		891.1			891.8
889.3			886.4		
885.7					875.0
875.0		874.6	869.3		
858.7	r5-t	858.1	854.5		
852.7			845.8	r6-t	848.8
812.9	r6-t	814.1	809.5	r7-t	811.4
776.4	r7-t	777.0	777.9	r8-t	778.8
759.7	r7-g		754.8	r9-t	754.0
751.7	r8-t	749.2	744.6	r9-g	
740.7	r8-g		740.2	r10-t	737.7
737.0	r9-t	734.3	732.1	r10-g	
731.5	r9-g	731.8	726.8	r11-t	725.3
729.0	r-g		721.9	r-g	
724.7	r10-t	721.8	718.4	r(CH_2)	717.4
718.2	r(CH_2)	716.6			

[a] r, ν_8 mode; t, straight chain; g, bent chain.

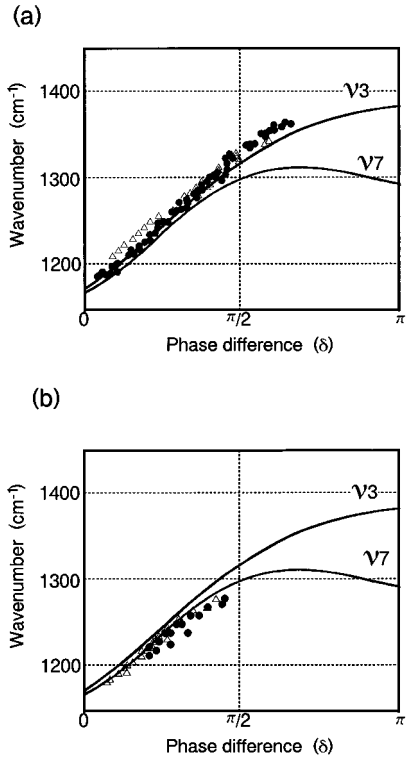

Figure 10. Frequency-phase difference curves for (a) ν_3 branch modes and (b) ν_7 branch modes for the β-forms of monoacid TAGs. The solid lines indicate the calculated dispersion curves for an infinite polymethylene chain.[23,24] Closed circles, straight *sn*-1,2 chains; open triangles, bent *sn*-3 chain.

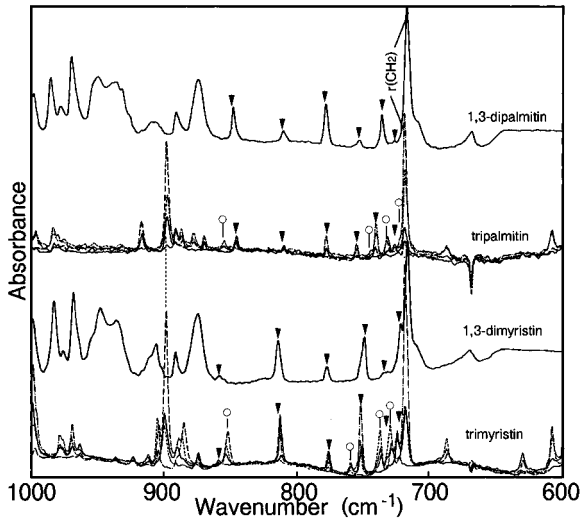

Figure 11. Normal incident transmission spectra of the β-forms of trimyristin, tripalmitin, 1,3-dimyristin, and 1,3-dipalmitin measured at 87 K. The relationship between the polarization of incident radiation and the crystal morphology in the polarized spectra of trimyristin and tripalmitin is the same as that in Figure 4. The bands marked with arrows are the ν_8 bands of the straight chains, and the bands with open circles are those of the bent chains.

chains, intense progression bands due to the ν_3 (CH_2 wagging) modes appear, while the ν_7 (CH_2 rocking−twisting) progression bands remain weak.

When an acyl chain takes a *gauche* conformation near the C−O bond, the ν(C−O) mode has both components parallel to the all-*trans* chain portion and perpendicular to the hydrocarbon zigzag plane. We consider that this results in the polarization changes of the ν_3 and ν_7 bands. First, the ν_3 progression bands coupled with the ν(C−O) mode show perpendicular polarization to some extent. In fact the ν_3 bands due to the bent chain appear stronger than those due to the straight chains in transmission spectra. Second, the intensities of the ν_7 progression bands increase, as described in the previous section. The ν(C−O) mode of the bent chain can couple strongly with the ν_7 branch modes, because the ν_7 modes contains the CH_2 rocking modes whose transition moments are perpendicular to the polymethylene zigzag plane. Therefore, the intensity borrowing from the ν(C−O) mode takes place.

2. Assignments of IR Bands in 1000−700 cm^{-1} Region. *Assignments of ν_7 Bands*. Figure 11 shows the normal incident transmission spectra (at 87 K) of trimyristin, tripalmitin, 1,3-dimyristin, and 1,3-dipalmitin. The frequencies of bands in this region are listed in Table 2. Since the spectra in the region of 1000−900 cm^{-1} are very complicated due to the overlapping of the ν_4 progression bands and CH_3 rocking modes, we focused on the assignment of the bands below 900 cm^{-1}. As we did in the assignments of the ν_3 and ν_7 bands, we have to take into account of the contribution of the straight *sn*-1,2 and the bent *sn*-3 chains, respectively. Therefore, we compared the spectra of TAGs with those of 1,3-DAGs in this region as shown in Figure 11. The marked bands with arrows in trimyristin and tripalmitin correspond to the bands in 1,3-DAGs. These bands can be assigned to the ν_8 progression of the straight *sn*-1,2 chains, and the other bands marked with open circles to those of the bent *sn*-3 chains.

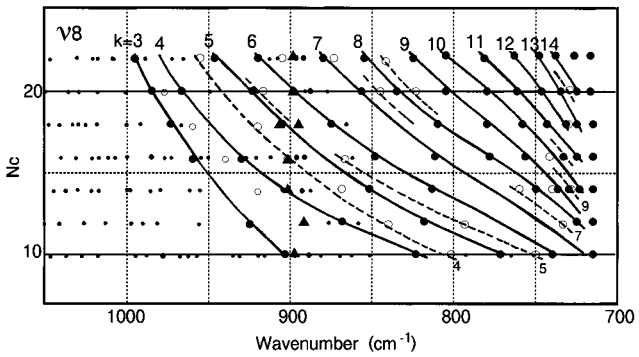

Figure 12. ν_8 branch mode array for monoacid TAGs. Solid lines, *sn*-1,2 chains; broken lines, *sn*-3 chain. Closed triangles stand for the band positions of methyl rocking modes ($r(CH_3)$).

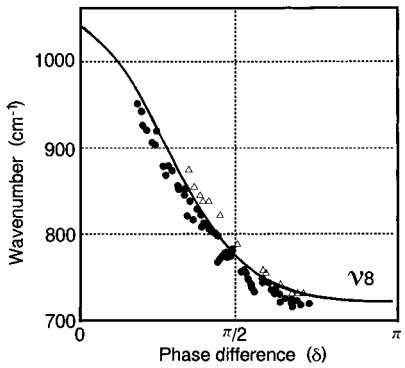

Figure 13. Frequency-phase difference curve for ν_8 branch modes. The solid line indicates the calculated dispersion curve for an infinite polymethylene chain.[23,24] Closed circles, bands due to the straight *sn*-1,2 chains; open triangles, bands due to the bent *sn*-3 chain.

In the same way, the bands of TAGs of tricaprin through tribehenin were analyzed by comparison with the bands of 1,3-DAGs of dilaurin through diarachidin. Figure 12 summarized the peak positions of the TAGs detectable in the transmission spectra taken at 87 K. The solid lines and dotted lines indicate the ν_8 bands of the straight *sn*-1,2 chains and the bent *sn*-3 chains, respectively.

Comparison of the Experimental Results with Theoretical Dispersion Curves. To confirm the assignments of the ν_8 progression bands, the observed frequency data were compared with the theoretical dispersion curve in Figure 13. The allowed phase angles, $\delta_{sn\text{-}1,2}$ and $\delta_{sn\text{-}3}$, were calculated using eqs 2 and 3. The *k* values were estimated by reference to the assignments of *n*-alkanes and *n*-alcohols and by considering the relation between the number of carbon atoms and frequencies as depicted in Figure 12. The experimental data well correspond to the theoretical dispersion curve for the ν_8 branch.

Conclusion

The CH_2 progression bands of the ν_3, ν_7, and ν_8 branches of monoacid TAG β-forms have been assigned. These progression bands include two components arising from (1) the straight *sn*-1,2 chains and (2) the bent *sn*-3 chain. It is noted that the progression bands of the bent chains greatly contribute to the intensity of bands, especially in the wagging region.

We consider that the assignments determined in this study are valuable information for solving the molecular configuration of TAGs in various aggregated states. In order to confirm the utility, we investigated the molecular structure of PPM (1,2-dipalmitoyl-3-myristoyl-*sn*-glycerol) in the β'_1-form. We treat the results in the following paper.

References and Notes

(1) Calaghan, P. T.; Jolly, K. W. *Chem. Phys. Lipids* **1977**, *19*, 56.
(2) Fahey, D. A.; Small, D. M. *Biochemistry* **1986**, *25*, 4468.
(3) Hagemann, J. W. *Crystallization and Polymorphism of Fats and Fatty Acids*; Garti, N., Sato, K. Eds.; Marcel Dekker: New York, 1988; pp 9−95.
(4) Small, D. M. *The Physical Chemistry of Lipids;* Plenum: New York, 1986; pp 345−394.
(5) Larsson, K. *Ark. Kemi* **1964**, *23*, 1.
(6) Jensen, L. H.; Mabis, A. J. *Acta Crystallogr.* **1966**, *21*, 770.
(7) Goto, M.; Kodali, D. R.; Small, D. M.; Honda, K.; Kozawa, K.; Uchida, T. *Proc. Natl. Acad. Sci. U.S.A.* **1992**, *89*, 9083.
(8) Kobayashi, M. In ref 3, pp 139−187.
(9) Kaneko, F.; Miyamoto, H.; Kobayashi, M. *J. Chem. Phys.* **1996**, *105*, 4812.
(10) Greenler, R. G. *J. Chem. Phys.* **1966**, *44*, 310.
(11) Allra, D. L.; Swalen, J. D. *J. Phys. Chem.* **1982**, *86*, 2700.
(12) Rabolt, J. F.; Burns, F. C.; Schlotter, N. E.; Swalen, J. D. *J. Chem. Phys.* **1983**, *78*, 946.
(13) Chapman, D. *J. Am. Oil. Chem. Soc.* **1964**, *42*, 353.
(14) Yano, J.; Ueno, S.; Sato, K.; Arishima, T.; Sagi, N.; Kaneko, F.; Kobayashi, M. *J. Phys. Chem.* **1993**, *97*, 12967.
(15) Ruig, W. G. *Appl. Spectrosc.* **1977**, *31*, 122.
(16) Barnes, J. D.; Fanconi, B. J. *J. Chem. Phys.* **1972**, *56*, 5190.
(17) Ewen, B.; Fisher, E. W.; Piesczek, W.; Strobl, G. *J. Chem. Phys.* **1974**, *61*, 5265.
(18) Zerbi, G.; Magni, R.; Gussoni, M.; Moritz, K. H.; Bigotto, A.; Dirlikov, S. *J. Chem. Phys.* **1981**, *75*, 3175.
(19) Maroncelli, M.; Strauss, H. L.; Snyder, R. G. *J. Chem. Phys.* **1985**, *82*, 2811.
(20) Kobayashi, M.; Kaneko, F.; Sato, K.; Suzuki, M. *J. Phys. Chem.* **1986**, *90*, 6371.
(21) Kim, Y.; Strauss, H. L.; Snyder, R. G. *J. Phys. Chem.* **1989**, *93*, 485.
(22) Snyder, R. G. *J. Mol. Spectrosc.* **1960**, *4*, 411.
(23) Snyder, R. G. *J. Mol. Spectrosc.* **1967**, *23*, 224.
(24) Tasumi, M.; Shimanouchi, T.; Miyazawa, T. *J. Mol. Spectrosc.* **1962**, *9*, 261.
(25) Tasumi, M.; Shimanouchi, T.; Watanabe, A.; Goto, R. *Spectrochim. Acta.* **1964**, *20*, 629.
(26) Fichmeister, I. *Prog. Chem. Fats Other Lipids* **1974**, *24*, 91.
(27) Larsson, K. *Acta Crystallogr.* **1971**, *B27*, 977.
(28) Larsson, K. *Acta Crystallogr.* **1963**, *16*, 741.
(29) Kaneko, F.; Shirai, O.; Miyamoto, H.; Kobayashi, M.; Suzuki, M. *J. Phys. Chem.* **1994**, *98*, 2185.
(30) Kaneko, F.; Ishikawa, E.; Kobayashi, M.; Suzuki, M. *Rep. Prog. Polym. Phys. Jpn.* **1994**, *37*, 241.
(31) Chia, Nian-Cherng; Mendelsohn, R. *J. Phys. Chem.* **1992**, *96*, 10543.